and mainly indicates that the methyl group is displaced slightly out of the ligand plane. In fact, the nonbounding interactomic distance between the methyl group and the nearest carbon atom of the benenzoid ring for PdTMTAA is 2.925 Å, about 0.2 Å shorter than the corresponding distance in the manganese compound. Thus, in PdTMTAA there exists comparatively little warping of the macrocyclic ligand, and the methyl groups tilt slightly from the plane of the macrocycle as they get closer to the benzenoid rings. Table VII also presents a comparison of some selected bond lengths. The bond lengths of the PdTMTAA molecule are similar to those of some of the previously characterized TMTAA's. The average C–N distance in the six-membered ring in PdTMTAA shows more double bond character. The average C–C distance in the six-membered chelate rings is comparable in all seven compounds. The average C–N distance on the five-membered chelate ring shows more single bond character in all seven compounds.

Thus, it has been shown that palladium coordination to the TMTAA ligand yields a unique geometry. The strain generated by this pseudoplanar geometry is not alleviated by increased bond lengths or warping. Only the slight displacement of the methyl groups out of the plane and the angular increase may account for this planarity. Such an effect might be explained in terms of an especially strong palladium coordination sphere. In order to maximize such interactions, the tetramethyltetraazaannulene ring distorts from its usually stable saddle shape. First-row transition-metal complexes of the TMTAA ligand exhibit this saddle shape. Perhaps extended interactions by the larger palladium d orbitals force the ligand into its pseudoplanar configuration.

Acknowledgment. The authors acknowledge support of this research project by the Office of Naval Research and the Robert A. Welch Foundation.

Registry No. PdTMTAA, 68833-19-2; PdTAA, 68833-20-5; bis(benzonitrile)palladous chloride, 14220-64-5.

Supplementary Material Available: A listing of observed and calculated structure factors (5 pages). Ordering information is given on any current masthead page.

References and Notes

(1) F. A. Cotton and G. Wilkinson, "Advanced Inorganic Chemistry", Interscience, New York, 1972, p 1031.
(2) D. W. Thomas and A. E. Martell, *J. Am. Chem. Soc.*, **81**, 5111 (1959).
(3) V. Eisner and M. J. C. Harding, *J. Chem. Soc.*, 4089 (1964).
(4) V. L. Goedken, J. J. Pluth, S.-M. Peng, and B. Bursten, *J. Am. Chem. Soc.*, **98**, 8014 (1976).
(5) H. Hiller, P. Dimroth, and H. Pfitzner, *Justus Liebigs Ann. Chem.*, **717**, 137 (1968).
(6) E.-G. Jäger, *Z. Anorg. Allg. Chem.*, **364**, 177 (1969).
(7) F. Hanic, M. Handlovic, and O. Lindgren, *Collect. Czech. Chem. Commun.*, **37**, 2119 (1972).
(8) V. L. Goedken, J. Molin-Case, and Y.-A. Wang, *J. Chem. Soc., Chem. Commun.*, 337 (1973).
(9) V. L. Goedken and Y.-A. Park, *J. Chem. Soc., Chem. Commun.* 214 (1975).
(10) D. R. Neves and J. C. Dabrowiak, *Inorg. Chem.*, **15**, 129 (1976).
(11) M. C. Weiss, B. Bursten, S.-M. Peng, and V. L. Goedken, *J. Am. Chem. Soc.*, **98**, 8021 (1976).
(12) R. Müller and D. Wöhrle, *Makromol. Chem.*, **176**, 2775 (1975).
(13) R. Müller and D. Wöhrle, *Makromol. Chem.*, **177**, 2241 (1976).
(14) L. G. Bell and J. C. Dabrowiak, *J. Chem. Soc., Chem. Commun.*, 512 (1975).
(15) G. C. Gordon, P. W. Dehaven, M. C. Weiss, and V. L. Goedken, *J. Am. Chem. Soc.*, **100**, 1003 (1978).
(16) M. Tsutsui, R. L. Bobsein, R. Pettersen, and R. Haaker, submitted for publication.
(17) F. Beck, W. Dammert, J. Heiss, H. Miller, and R. Polster, *Z. Naturforsch.*, **28**, 1009 (1973).
(18) H. Alt, H. Binder, and G. Sandstede, *J. Catal.*, **28**, 8 (1973).
(19) F. Beck, *Ber. Bunsenges. Phys. Chem.*, **77**, 353 (1973).
(20) D. P. Fisher, V. Piermattie, and J. C. Dabrowiak, *J. Am. Chem. Soc.*, **99**, 2811 (1977).
(21) M. C. Weiss, G. Gordon, and V. L. Goedken, *Inorg. Chem.*, **16**, 305 (1977), and references cited therein.
(22) W. H. Woodruff, R. W. Pastor, and J. C. Dabrowiak, *J. Am. Chem. Soc.*, **98**, 7999 (1976).
(23) F. C. McElroy and J. C. Dabrowiak, *J. Am. Chem. Soc.*, **98**, 7112 (1976).
(24) M. S. Kharasch, R. C. Seyler, and F. R. Mayo, *J. Am. Chem. Soc.*, **60**, 882 (1938).
(25) Elemental analyses were performed by Schwarzkopf Microanalytical Laboratory, Woodside, NY 11377.
(26) Center for Trace Characterization, Texas A&M University, College Station, TX 77843.
(27) Infrared and mass spectral results are also consistent.
(28) "International Tables for X-ray Crystallography", Vol. 4, Kynoch Press, Birmingham, England, 1974.
(29) D. T. Cromer and D. Liberman, *J. Chem. Phys.*, **53**, 1891 (1970).
(30) E. B. Fleischer, C. K. Miller, and L. E. Webb, *J. Am. Chem. Soc.*, **86**, 2342 (1964).
(31) L. Pauling, "The Nature of the Chemical Bond", Cornell University Press, Ithaca, NY, 1960, p 518.

Contribution from the Department of Chemistry, Pacific Lutheran University, Tacoma, Washington 98447,
and the Chemical Physics Program, Washington State University, Pullman, Washington 99164

Crystal Structure and Magnetic Susceptibility of Di-μ-chloro-bis[chlorobis(tetramethylene sulfoxide)copper(II)], $Cu_2Cl_4(C_4H_8SO)_4$: An Antiferromagnetic Dimer

DUANE D. SWANK,* GREGORY F. NEEDHAM, and ROGER D. WILLETT

Received July 13, 1978

Crystals of $Cu_2Cl_4(C_4H_8SO)_4$ belong to the monoclinic space group $P2_1/c$ (C_{2h}^5) with lattice constants $a = 9.205$ (1) Å, $b = 14.614$ (9) Å, $c = 9.660$ (4) Å, $\beta = 84.629$ (3)°, $Z = 4$, $D_{\text{calcd}} = 1.76$ g/cm^3 and $D_{\text{measd}} = 1.77$ (2) g/cm^3. A room-temperature, single-crystal X-ray diffraction study was performed along with a study of the magnetic susceptibility from 4 up to 110 K. The structure was solved by direct methods and refined by full-matrix least-squares techniques to $R(F_o) = 0.049$ for 1544 unique reflections. The copper ion in each *trans*-$CuCl_2(C_4H_8SO)_2$ monomer has a significant tetrahedral distortion from planarity. Long Cu–Cl interactions between monomer units create discrete bibridged dimeric species. The copper–chlorine–copper bridging geometry is asymmetric with one long bond (3.020 Å) and one short bond (2.270 Å); the bridging angle is 88.5°. Magnetic susceptibility measurements over the temperature range 4–110 K show the salt is antiferromagnetically coupled ($J/k = -12$ K). Similarly, EPR measurements indicate weak interdimer interactions ($J'/k \approx 0.1$ K) also exist.

Introduction

Interest in the role of ligand characteristics such as size and geometry in determining magnetic interactions between metal ions has increased in recent years. The role of the ligand in determining bond angles and distances in bridging moieties and interchain exchange pathways lead to the investigation of a series of compounds of copper chloride with dimethyl sulfoxide ($(CH_3)_2SO$) and tetramethylene sulfoxide ((C-

---

*To whom correspondence should be addressed at Washington State University.

0020-1669/79/1318-0761$01.00/0

Table I. Atomic Parameters for $Cu_2Cl_4((CH_2)_4SO)_4$[a,b]

atom	x	y	z	B_{11}	B_{22}	B_{33}	B_{12}	B_{13}	B_{23}
Cu	0.8504 (1)	0.4719 (1)	0.6376 (1)	0.0107 (1)	0.0033 (1)	0.0081 (1)	−0.0010 (1)	−0.0032 (1)	0.0009 (1)
Cl1	0.9224 (2)	0.6151 (1)	0.5669 (1)	0.0123 (2)	0.0030 (1)	0.0098 (2)	−0.0007 (1)	−0.0027 (1)	0.0008 (1)
Cl2	0.6946 (2)	0.3889 (1)	0.7842 (1)	0.0138 (2)	0.0056 (1)	0.0103 (2)	−0.0019 (1)	−0.0006 (2)	0.0018 (1)
S1	1.0459 (2)	0.3617 (1)	0.7935 (1)	0.0120 (2)	0.0033 (1)	0.0075 (2)	0.0006 (1)	−0.0026 (1)	−0.0002 (1)
S2	0.7049 (1)	0.3580 (1)	0.4424 (1)	0.0105 (2)	0.0037 (1)	0.0086 (2)	−0.0008 (1)	−0.0026 (1)	0.0003 (1)
O1	1.0038 (4)	0.4618 (2)	0.7630 (3)	0.0126 (5)	0.0032 (2)	0.0091 (4)	−0.0002 (2)	−0.0038 (4)	0.0006 (2)
O2	0.7280 (4)	0.4589 (2)	0.4852 (3)	0.0114 (5)	0.0034 (2)	0.0089 (4)	−0.0002 (2)	−0.0039 (4)	−0.0000 (2)
C1	1.2758 (9)	0.3986 (6)	0.9317 (8)	0.0156 (12)	0.0075 (5)	0.0163 (10)	−0.0004 (6)	−0.0071 (9)	0.0005 (6)
C2	1.0233 (7)	0.3529 (4)	0.9816 (6)	0.0167 (11)	0.0041 (3)	0.0079 (7)	0.0017 (5)	0.0018 (7)	0.0009 (4)
C3	1.2414 (7)	0.3670 (5)	0.7894 (7)	0.0114 (9)	0.0064 (4)	0.0111 (8)	0.0021 (5)	0.0002 (7)	0.0001 (5)
C4	1.1727 (8)	0.3503 (5)	1.0352 (7)	0.0209 (13)	0.0066 (5)	0.0095 (8)	0.0007 (6)	−0.0048 (8)	−0.0002 (5)
C5	0.5114 (7)	0.3493 (5)	0.4302 (7)	0.0102 (9)	0.0076 (5)	0.0122 (9)	−0.0034 (5)	−0.0000 (7)	−0.0014 (5)
C6	0.7429 (7)	0.3589 (5)	0.2564 (6)	0.0126 (10)	0.0059 (4)	0.0080 (6)	−0.0005 (5)	0.0005 (7)	−0.0018 (4)
C7	0.6014 (18)	0.3662 (15)	0.1945 (12)	0.0174 (15)	0.0244 (19)	0.0092 (11)	−0.0020 (13)	−0.0055 (11)	0.0023 (10)
C8	0.4829 (13)	0.3719 (9)	0.2891 (13)	0.0101 (13)	0.0298 (19)	0.0160 (13)	0.0031 (14)	−0.0045 (11)	0.0050 (15)

atom	x	y	z	B, Å^2	atom	x	y	z	B, Å^2
C1H1	1.224 (10)	0.460 (7)	0.958 (9)	8.0	C5H1	0.521 (11)	0.375 (7)	0.487 (10)	8.0
C1H2	1.373 (11)	0.491 (6)	0.955 (9)	8.0	C5H2	0.524 (10)	0.287 (7)	0.449 (9)	8.0
C2H1	0.951 (10)	0.405 (7)	0.914 (9)	8.0	C6H1	0.697 (11)	0.314 (7)	0.285 (10)	8.0
C2H2	0.969 (10)	0.305 (6)	1.004 (9)	8.0	C6H2	0.678 (10)	0.397 (7)	0.254 (9)	8.0
C3H1	1.260 (11)	0.315 (7)	0.779 (10)	8.0	C7H1	0.604 (22)	0.359 (13)	0.156 (17)	8.0
C3H2	1.275 (11)	0.396 (7)	0.711 (10)	8.0	C7H2	0.605 (11)	0.389 (7)	0.090 (10)	8.0
C4H1	1.168 (10)	0.379 (6)	1.126 (10)	8.0	C8H1	0.522 (17)	0.394 (9)	0.270 (16)	8.0
C4H2	1.207 (10)	0.276 (7)	1.020 (9)	8.0	C8H2	0.386 (11)	0.386 (6)	0.265 (9)	8.0

[a] Uncertainties in last digit are given in parentheses. [b] Thermal parameters are defined by $T = \exp[-(B_{11}h^2 + B_{22}k^2 + B_{33}l^2 + 2B_{12}hk + 2B_{13}hl + 2B_{23}kl)]$.

$H_2)_4SO)$ as ligands. These produce low-symmetry complexes with unusual coordination geometries. In addition, the existence of Cu–L–Cu bridges produces systems with interesting magnetic properties. In particular, the $CuCl_2{\cdot}(CH_3)_2SO$ and $CuCl_2{\cdot}(CH_2)_4SO$ salts are the first examples of spin $^1/_2$ Heisenberg linear-chain magnetic systems.[1,2] In these salts, two Cu–Cl–Cu bridges (one symmetrical and one asymmetrical) and one asymmetric Cu–O–Cu bridge exist.[3] Thus the sulfoxide is coordinated to two metal centers with one short Cu–O distance (1.9 Å) and one very long Cu–O distance (3.1 Å). With the tetramethylene sulfone ($(CH_2)_4SO_2$) ligand in $Cu_3Cl_6(H_2O)_2{\cdot}2(CH_2)_4SO_2$[4] only one weak Cu–O interaction occurs; the other oxygen of the sulfone group is hydrogen bonded to the water molecule. Finally, in $CuX_2{\cdot}2(CH_3)_2SO$ (X = Cl, Br)[5,6] a distorted five-coordinate geometry is obtained about the copper ion, the geometry being intermediate between square pyramidal and trigonal bipyramidal. In order to further probe the variations of these systems, we have undertaken a structural and magnetic investigation of $CuCl_2{\cdot}2(CH_2)_4SO$.

Experimental Section

Structural Data. The compound was prepared by adding tetramethylene sulfoxide ($(CH_2)_4SO$) to 50 mL of 1-propanol at 70 °C. Then anhydrous $CuCl_2$ was added in a 1:2 mole ratio. The resulting solution was heated for 2 h and then cooled slowly. The crystals were filtered and washed with cold 1-propanol. Anal. Calcd: C, 28.03; H, 4.70. Found: C, 27.75; H, 4.60.

Systematic extinctions for the monoclinic crystal ($h0l$, $l = 2n + 1$, and $0k0$, $k = 2n + 1$) indicated the correct space group to be $P2_1/c$. The density, based on flotation techniques, is 1.76 g/cm^3. The calculated density for $Z = 4$ is 1.77 g/cm^3. The crystal selected for data collection was shaped into a sphere with a diameter of 0.37 mm. Intensity data were collected on an automated Picker full-circle diffractometer with Zr-filtered Mo Kα radiation. A total of 1544 unique reflections were collected in the range $5° \leq 2\theta \leq 45°$ using a θ–2θ scan with a scan width of 2.4° with 20 steps/deg and 2.0 s/step. Background was counted on each side of the reflection for 10 s. The standard deviation of each reflection was calculated by $\sigma^2(I) = \mathrm{TC} + \mathrm{BG} + 0.03^2I^2$, corrected for counting time, where TC = total counts, BG = background counts, and $I = \mathrm{TC} - \mathrm{BG}$. The intensities of three reflections were monitored every 80 reflections to check for crystal decomposition, etc. The standards deviated only 1% throughout the data collection. Absorption corrections were not made ($\mu = 24.5$ cm^{-1}).

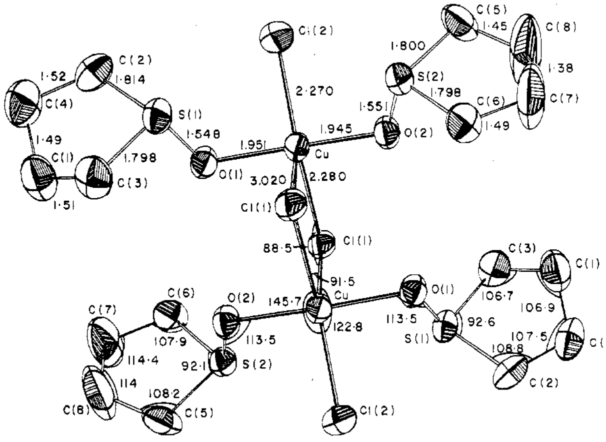

Figure 1. Illustration of the $Cu_2Cl_4{\cdot}4(CH_2)_4SO$ dimer unit.

Structure Solution and Refinement. The noncarbon and nonhydrogen atoms were located by the program MULTAN.[7] The carbon positions were located from a Fourier map, and the hydrogen positions were calculated. Refinement was completed using first isotropic and then anisotropic thermal parameters on all nonhydrogen atoms. The thermal parameters on the hydrogens were fixed at 8.0 Å^2. The refinement converged to a value of R_2 [$= [\sum w(|F_o| - |F_c|)^2/\sum w|F_o|^2]^{1/2}$] of 4.9%. R_1 [$= \sum||F_o| - |F_c||/\sum|F_o|$], omitting reflections whose intensities were less than 3σ, was 3.7%. Maximum parameter shifts on the last cycle of refinement were less than their estimated errors. Scattering factor tables for Cu^{2+}, Cl^-, S, O, C, and H were taken from ref 8. Computer programs used were part of a local library.[9] Final parameters are given in Table I, and bond distances and angles are given in Table II and illustrated in Figure 1.

Results and Discussion

Crystal Structure. The structure consists of discrete copper dimers composed of two *trans*-$CuCl_2((CH_2)_4SO)_2$ monomer moieties. One of the chlorine atoms, Cl(1), in each monomer interacts with the adjacent copper to form the asymmetric bibridged dimer unit shown in Figure 1. The Cu_2Cl_2 bridging unit is characterized by Cu–Cl distances of 2.280 and 3.020 Å and a Cu–Cl–Cu angle of 88.5°. The resultant copper coordination geometry is best described as square pyramidal,

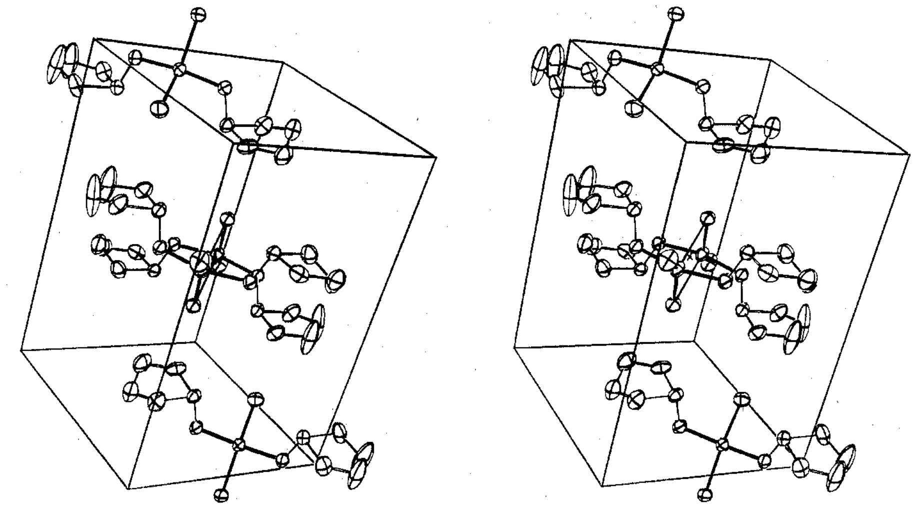

Figure 2. Stereoscopic view of the unit cell of $Cu_2Cl_4{\cdot}4(CH_2)_4SO$. The origin of the unit cell is at the center of the figure, with the *b* axis vertical and the *c* axis receding into the paper.

Table II. Interatomic Distances (Å) and Bond Angles (deg) for $Cu_2Cl_4(C_4H_8SO)_4$

(a) Distances around the Copper Atom			
Cu-Cl(1)	2.280 (2)	Cu-O(2)	1.945 (4)
Cu-Cl(2)	2.270 (2)	Cu-Cl(1^a)	3.020 (2)
Cu-O(1)	1.951 (4)	Cu-Cu^a	3.737 (2)
(b) Angles around the Copper Atom			
Cl(1)-Cu-Cl(1^a)	91.5 (1)	Cl(1)-Cu-O(2)	92.1 (1)
Cl(1)-Cu-Cl(2)	145.7 (1)	Cl(1^a)-Cu-O(2)	83.0 (1)
Cl(1^a)-Cu-Cl(2)	122.8 (1)	Cl(2)-Cu-O(1)	91.4 (1)
Cl(1)-Cu-O(1)	92.8 (1)	Cl(2)-Cu-O(2)	92.5 (1)
Cl(1^a)-Cu-O(1)	82.9 (1)	O(1)-Cu-O(2)	165.2 (1)
(c) S-O Distances in the Sulfoxide Groups			
S(1)-O(1)	1.548 (4)	S(2)-O(2)	1.551 (4)
(d) Cu-O-S Angles in the $(CH_2)_4SO$ Groups			
Cu-O(1)-S(1)	113.5 (2)	Cu-O(2)-S(2)	113.5 (2)
(e) Distances within the Sulfoxide Rings			
S(1)-C(2)	1.814 (6)	S(2)-C(5)	1.800 (7)
S(1)-C(3)	1.798 (7)	S(2)-C(6)	1.798 (6)
C(1)-C(3)	1.51 (1)	C(5)-C(8)	1.45 (1)
C(1)-C(4)	1.49 (1)	C(6)-C(7)	1.49 (2)
C(2)-C(4)	1.52 (1)	C(7)-C(8)	1.36 (2)
(f) Angles within the Sulfoxide Rings			
C(2)-S(1)-C(3)	92.6 (3)	C(5)-S(2)-C(6)	92.1 (3)
S(1)-C(3)-C(1)	106.7 (5)	S(2)-C(5)-C(8)	108.2 (6)
C(3)-C(1)-C(4)	106.9 (6)	C(5)-C(8)-C(7)	114.4 (10)
C(1)-C(4)-C(2)	107.5 (6)	C(8)-C(7)-C(6)	114.4 (9)
C(4)-C(2)-S(1)	108.8 (4)	C(7)-C(6)-C(2)	107.9 (7)
(g) Oxygen-Sulfur-Carbon Angles in the Sulfoxide Groups			
O(1)-S(1)-C(2)	104.5 (2)	O(2)-S(2)-C(5)	104.2 (3)
O(1)-S(1)-C(3)	102.9 (3)	O(2)-S(2)-C(6)	103.9 (3)
(h) Intermolecular Contacts			
S(1)-Cl(1^b)	3.869 (3)	O(1)-S(1)-Cl(1^b)	167.1 (2)
S(2)-Cl(2^c)	3.923 (3)	O(2)-S(2)-Cl(2^c)	170.7 (1)
(i) Intradimer Contacts			
Cu-Cu^a	3.736 (2)	C(1)-C(7^a)	3.78 (2)
O(1)-O(2^a)	3.477 (5)	C(1)-C(6^a)	3.99 (1)
O(1)-C(6^a)	3.502 (8)	C(3)-C(6^a)	4.03 (1)
O(2)-C(3^a)	3.668 (8)		

[a] Symmetry transformation: $2-x$, $1-y$, $1-z$. [b] Symmetry transformation: $2-x$, $^1/_2-y$, $^3/_2-z$. [c] Symmetry transformation: x, $^1/_2-y$, $-^1/_2+z$.

although the basal group shows a significant distortion toward a tetrahedral configuration. The basal Cu–Cl distances are 2.270 and 2.280 Å, while the Cu–O distances are 1.945 and 1.951 Å. However, unlike typical square-pyramidal complexes, the Cu ion does not sit above the basal plane. Rather the cis Cl–Cu–O angles (91.4–92.8°) are all larger than 90°, indicating the presence of a tetrahedral distortion. This tetrahedral distortion yields a Cl–Cu–Cl angle of 145.7° and an O–Cu–O angle of 165.2° as seen in the stereoscopic illustration in Figure 2. The fifth atom nominally within the coordination sphere, Cl(1) from the adjacent monomer, is at a distance of 3.02 Å. At this distance, all contacts of this bridging chlorine with atoms in the basal plane are greater than the sum of the van der Waals radii.

Table III. Comparison of Coordination Geometry in $CuCl_2{\cdot}2(CH_2)_4SO$ and $CuCl_2{\cdot}2(CH_3)_2SO$

	$(CH_2)_4SO$	$(CH_3)_2SO$
Cu-O, Å	1.948	1.955
Cu-Cl(t),[a] Å	2.280	2.284
Cu-Cl(b), Å	2.270	2.290
Cu-Cl(b), Å	3.020	2.702
O-Cu-O, deg	165.2	173.0
Cl(t)-Cu-Cl(b), deg	145.7	146.1
Cl(t)-Cu-Cl(b), deg	122.8	112.7
Cl(b)-Cu-Cl(b), deg	91.5	101.2

[a] t designates terminal chlorine; b denotes bridging chlorine.

The most significant intradimer contacts are given in Table II. These dictate the long Cu–Cl distance between monomers and therefore prevent the monomers from approaching each other more closely. This, in turn, allows the $CuCl_2((CH_2)_4SO)_2$ moiety to distort toward tetrahedral geometry. This type of 4 + 1 geometry exists in $[(CH_3)_2CHNH_3]_2CuCl_4$,[10] but its significance was not recognized. It is also present, although to a lesser extent, in the $CuX_2{\cdot}2(CH_3)_2SO$[6,7] salts (X–Cu–X = 146°, O–Cu–O = 173°, Cu–Cl′ = 2.702 Å, Cu–Br′ = 2.777 Å) and in $[Co(en)_3]_2(Cu_2Cl_8)Cl_2{\cdot}2H_2O$ (Cl–Cu–Cl = 145.3 and 172.6°, Cu–Cl′ = 2.703 Å).[11] Thus, we can use these data to visualize a pathway for the interaction of a chloride ion with a tetrahedral $CuCl_4^{2-}$ ion to form the trigonal-bipyramidal $CuCl_5^{2-}$ species. The usual picture of formation of the trigonal-bipyramidal $CuCl_5^{3-}$ ion starts with square-planar $CuCl_4^{2-}$ and proceeds through a square-pyramidal intermediate. In contrast, on the basis of the structure, we can start with a normal "tetrahedral" $CuCl_4^{2-}$ ion with a trans Cl–Cu–Cl angle near 130°. The approach of the fifth chloride ion forces one angle toward 180°. Simultaneously, the other trans angle opens up toward the commonly observed angle near 145°. Then, as the Cu–Cl′ bond shortens toward the equatorial length of 2.4 Å, Cl–Cl repulsion forces the latter back to 120°, giving the trigonal-bipyramidal geometry.

The planes of the $(CH_2)_4SO$ rings are approximately perpendicular to the plane of the copper dimers (dihedral

Table IV. Magnetic Susceptibility Data for $Cu_2Cl_4(C_4H_8SO)_4$

T	$10^2\chi$/mol[a]	T	$10^2\chi$/mol
4.126	0.167	17.630	1.350
4.512	0.162	18.635	1.346
4.673	0.215	19.672	1.281
5.356	0.314	20.314	1.302
5.382	0.333	21.245	1.309
5.881	0.364	22.640	1.223
6.344	0.445	24.170	1.161
6.391	0.478	25.503	1.125
7.045	0.598	27.251	1.093
7.252	0.681	29.631	1.025
7.259	0.658	31.255	1.004
7.716	0.759	34.474	0.941
8.302	0.848	35.335	0.922
8.952	0.955	38.557	0.867
9.356	1.015	43.110	0.800
10.529	1.159	46.813	0.751
11.960	1.234	53.119	0.677
12.990	1.313	60.402	0.602
12.600	1.305	66.959	0.550
13.676	1.345	73.860	0.501
14.438	1.358	83.729	0.450
15.515	1.376	89.856	0.422
16.498	1.366	90.112	0.421
17.051	1.332	101.167	0.379

[a] In cgsu.

angles are 80.38 and 86.09°). The $(CH_2)_4SO$ groups occupy cis positions with respect to the dimer plane. This is in contrast to the trans configuration predicted to minimize steric hindrance. The C_4S ring associated with S(1) has normal distances and angles. However, it is clear from the amplitudes of thermal motion and the small deviation from planarity of the ring associated with S(2) that it is disordered. The averaging of the two forms of the ring conformations leads to shortened C–C distances and enlarged C–C–C angles.

The unit cell, illustrated in Figure 2, is composed of dimers located at the origin and the body center. The dimers are displaced from each other in the cell such that the $(CH_2)_4SO$ ring of one dimer lies above the Cu–Cl rectangle of the central dimer. The interdimer Cl–S distances (i.e., the approximate separation of the dimer and the $(CH_2)_4SO$ ring) are 3.869 and 3.923 Å.

Magnetic Susceptibility and ESR Measurements. Magnetic susceptibility measurements were made on a 105.4-mg sample with a PAR vibrating-sample magnetometer over the temperature range 4–110 K. A field of 5094 Oe was used and the temperature was measured with a carbon-glass resistance thermometer. Details of temperature calibration will be published later. ESR measurements were made at 9 and 36 GHz. The susceptibility data, corrected for diamagnetic and TIP contributions, are tabulated in Table IV.

In light of the structural results, the susceptibility data were analyzed in terms of the Heisenberg dimer model. As seen in Figure 3, this gives a very satisfactory fit with an antiferromagnetic coupling, $2J/k = -24$ K. The largest deviation between theory and experiment lies in the temperature regime where χ is a maximum. Unfortunately, the uncertainties in a rather large background moment were a maximum at these temperatures and account for the discrepancy. This leads to an uncertainty of $2J/k$ of ±1 K.

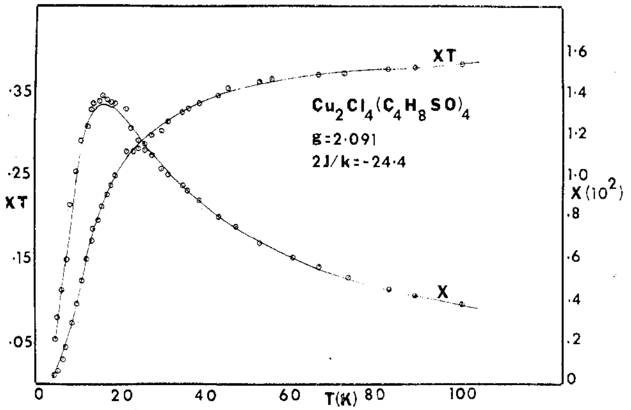

Figure 3. Plots of the susceptibility, χ (right-hand ordinate), and of χT (left-hand ordinate) vs. T.

The ESR spectrum of single crystals of $CuCl_2{\cdot}2(CH_2)_4SO$ at both 9 and 36 GHz consists of a single exchange-narrowed resonance line in all orientations. It is not a typical dimer spectrum and, in particular, no $\Delta S = \pm 2$ line is observed at half-field. Thus, significant interdimer coupling exists. The EPR line widths are not the same at 9 and 36 GHz. In principle, the frequency dependence can be used to estimate the magnitude of the interdimer coupling, J', since this coupling averages the **g** tensors of magnetically inequivalent ions and the effective averaging will depend on the ratio $(H_1 - H_2)/J'$, where H_1 and H_2 are the resonance fields of the inequivalent ions. However, we see a frequency dependence in the *ac* plane, where all ions are equivalent. Thus, other processes are contributing to the observed frequency dependence. We have made no attempt to analyze this phenomenon at this time, but we consider it likely that $J' \approx (\Delta g/g)\hbar\omega$ or $J'/k \approx 0.1$ K. It was also impossible to estimate this from the χ data because of the strong coupling between J' and g. The source of this interdimer interaction is probably the S–Cl contacts of 3.9 Å. This order of magnitude of exchange is reasonable in light of the unfavorable orientation of the Cl atoms with respect to the sulfur lone pairs (O–S–Cl ≈ 170°). In $CuCl_2{\cdot}(CH_3)_2SO$ and $CuCl_2{\cdot}(CH_2)_4SO$, interchain S–S contacts of 3.67 Å with more favorable orientation (O–S–S ≈ 120°) give values of $J'/k \approx 1$ K.

Comparison of Structural and Magnetic Data. Hatfield has recently summarized much of the known magnetic data on salts containing asymmetrical Cu–Cl bridges.[12] Table V compares $Cu_2Cl_4((CH_2)_4SO)_4$ with other dimers. In contrast to the symmetrical hydroxy-bridge species,[13] no clear structural–magnetic correlations exist. This is not surprising since we are not dealing with a one-parameter problem (the Cu–L–Cu bridging angle, θ); in addition to θ, J depends upon such variables as the axial Cu–Cl distance, the Cu–Cu distance, and the distortions of the coordination geometry from planarity. It is worthwhile making the following observations. The bridging geometry in $CuCl_2{\cdot}2(CH_2)_4SO$ is almost identical with that in the $CuCl_2{\cdot}2py$ linear chain (Cu–Cl = 2.30 Å,

Table V. Magnetic and Structural Data for Chloro-Bridged Copper(II) Dimers[12]

complex	$2J$, cm^{-1}	structure	Cu–Cl–Cu, deg	Cu–Cl bond, Å in-plane	Cu–Cl bond, Å out-of-plane	Cu–Cu dist, Å
$[(guaninium)CuCl_3]_2{\cdot}2H_2O$	−82.6	trigonal-bipyramidal	98	2.45	2.29	3.58
$[Cu_2Cl_8]^{4-}$ anion	−14.6	trigonal-bipyramidal	95.2	2.70	2.33	3.72
$[(2\text{-Mepy})_2CuCl_2]_2$[a]	−7.4	square-pyramidal	101.4	2.26	3.37	4.41
$[(DMG)CuCl_2]_2$[b]	+6.3	square-pyramidal	88	2.24	2.70	3.44
$CuCl_2{\cdot}2(CH_2)_4SO$	−16.0	square-pyramidal	88.5	2.28	3.02	3.74

[a] 2-Mepy = 2-methylpyridine. [b] DMG = dimethylgloxime.

Cu···Cl = 3.02 Å, θ = 91.5°). Since J is not expected to be extremely sensitive to θ, we can reasonably compare the two exchange constants, −12 and −13.4 K, respectively, based only on the coordination geometry. Thus, the distortion from planar coordination present in $CuCl_2 \cdot 2(CH_2)_4SO$ (but not in $CuCl_2 \cdot 2py$) causes a decrease in the antiferromagnetic coupling. This is not surprising since, with the lobes of the $d_{x^2-y^2}$ orbital not pointing directly at the chlorine atoms, lower electron density is anticipated at the bridging chlorine and thus less exchange of spin information. Likewise, the dimethylglyoxime complex $[(DMG)CuCl_2]_2$ has nearly identical bridging geometry (Cu–Cl = 2.24 Å, Cu···Cl = 2.70 Å, θ = 88°) except for the 0.3-Å shortening of the long Cu–Cl bond. Yet this shortening has the effect of changing the interaction from antiferromagnetic to ferromagnetic ($J/k = -12$ vs. +4.4 K)! Finally, we note that the linear-chain arrangement in $CuCl_2 \cdot 2(CH_3)_2SO$ leads to weak antiferromagnetic interaction ($J/k = -4.8$ K).[14] In this salt, a monobridged superexchange pathway exists, with θ = 144.6°.

Summary

We have shown that discrete $Cu_2Cl_4(C_4H_8SO)_4$ dimers exist in the solid state in the 2:1 $(CH_2)_4SO–CuCl_2$ salt. The coordination geometry, approximately square pyramidal, contains three chlorine and two oxygen atoms. Copper atoms within the dimer are linked by a pair of asymmetrical Cu–Cl···bridges, leading to antiferromagnetic coupling with a singlet–triplet separation of 24 K.

Acknowledgment. We thank C. P. Landee for assistance with the susceptibility measurements and R. Wong for the EPR measurements. The work was supported by NSF.

Registry No. $Cu_2Cl_4((CH_2)_4SO)_4$, 68876-53-9.

Supplementary Material Available: A listing of observed and calculated structure factors (5 pages). Ordering information is given on any current masthead page.

References and Notes

(1) D. D. Swank, C. Landee, and R. D. Willett, *J. Appl. Phys.*, **49**, 1329 (1978).
(2) C. Landee and R. D. Willett, Abstracts, Northwest Regional Meeting of the American Chemical Society, Seattle, Wash., 1978; Abstract No. 135.
(3) D. D. Swank, C. Landee, and R. D. Willett, *Phys. Rev. B*, submitted for publication.
(4) D. D. Swank and R. D. Willett, *Inorg. Chim. Acta*, **8**, 143 (1974).
(5) R. D. Willett and K. Chang, *Inorg. Chim. Acta*, **4**, 447 (1970).
(6) F. Jardine, S. A. Roberts, and R. D. Willett, *Inorg. Chim. Acta*, **25**, 97 (1977).
(7) G. Germain, P. Main, and M. M. Woolfson, *Acta Crystallogr., Sect. A*, **27**, 368–376 (1971).
(8) "International Tables for X-Ray Crystallography", Vol. III, Kynoch Press, Birmingham, England, 1962.
(9) This includes modified versions of the following: Busing, Martin, and Levy's ORFLS least-squares program; Hubbard, Quicksall, and Jacobson's ALFF Fourier program; the function and error program, ORFFE, by Busing, Martin, and Levy; Johnson's ORTEP program for crystallographic illustrations; and the absorption correction subroutine ORABS by Wehe, Busing, and Levy.
(10) D. N. Anderson and R. D. Willett, *Inorg. Chim. Acta*, **8**, 167 (1974).
(11) D. J. Hodgson, P. K. Hale, and W. E. Hatfield, *Inorg. Chem.*, **10**, 1061 (1971).
(12) V. H. Crawford and W. E. Hatfield, *Inorg. Chem.*, **16**, 1336 (1977); W. E. Hatfield, *ACS Symp. Ser.*, **No. 5**, 108 (1974).
(13) V. H. Crawford, H. W. Richardson, J. R. Wasson, D. J. Hodgson, and W. E. Hatfield, *Inorg. Chem.*, **15**, 2107 (1976).
(14) N. T. Wadkins, D. Y. Jeter, S. M. Horner, and W. E. Hatfield, *Trans. Faraday Soc.*, **67**, 2431 (1971).

Contribution from the Department of Chemistry
and Ames Laboratory—DOE, Iowa State University, Ames, Iowa 50011

Preparation, Structure, and Spectral Characterization of Bis[D-β-(2-pyridyl)-α-alaninato]cobalt(III), $Co(D\text{-}Pyala)_2^+$

STEPHEN R. EBNER, ROBERT A. JACOBSON, and ROBERT J. ANGELICI*

Received July 21, 1978

The complex $[Co(D\text{-}Pyala)_2]NO_3 \cdot {}^1/_2H_2O$ was prepared by reaction of Co(II) or Co(III) with D-$H_2NCH(CH_2C_5H_4N)CO_2^-$, D-Pyala⁻, the tridentate analogue of histidine. It was established by an X-ray crystal study of the complex that of the three possible isomeric forms, the most stable was that in which the carboxylate groups of the two ligands are mutually trans. This structure contrasts with that of the predominant isomer of the histidinate complex $Co(L\text{-}his)_2^+$, in which the imidazole groups are mutually trans. Infrared, ^1H NMR, visible, ORD, and CD spectra of $Co(D\text{-}Pyala)_2^+$ are discussed and are entirely consistent with the solid-state structure.

Introduction

The synthetic amino acid β-(2-pyridyl)-α-alanine, $^+H_3NCH\text{-}(CH_2C_5H_4N)CO_2^-$ (PyalaH), is a tridentate analogue of histidine with a pyridine group in place of the imidazole. In earlier work, it was shown that Pyala⁻ binds to transition-metal ions to form $M(Pyala)_2$ with some enantioselectivity depending upon the chirality of the Pyala⁻ ligand.[1] Where the ligand is present as only one enantiomer, e.g., D-Pyala⁻, the octahedral $M(D\text{-}Pyala)_2$ complexes may exist in three geometric isomeric forms (Figure 1). In the present study, we prepared the Co(III) complex $Co(D\text{-}Pyala)_2^+$ for the purpose of establishing the most stable isomer of this complex.

All three isomers of the $Co(ligand)_2^+$ complexes have been isolated for the tridentate ligands L-histidinate[2,3], L-2,3-diaminopropionate,[4] and L-2,4-diaminobutyrate.[5] The trans-imidazole isomer was the major structural form of $Co(L\text{-}his)_2^+$. It was suggested that because of steric hindrance the imidazole groups prefer to occupy trans positions in octahedral $M(his)_2$ complexes.[6] Because of the similarity of Pyala⁻ to his⁻, $Co(D\text{-}Pyala)_2^+$ might be expected to prefer the trans-pyridyl structure. However, as reported herein, the trans-carboxylate structure is the most stable form. This complex was fully characterized by its IR, ^1H NMR, visible, ORD, and CD spectra.

Experimental Section

Materials. Racemic β-(2-pyridyl)-α-alanine (PyalaH) was prepared and resolved as described previously.[7] $[Co(NH_3)_4CO_3]NO_3$,[8a] $[Co(NH_3)_6](NO_3)_3$,[8b] and $Na_3[Co(CO_3)_3] \cdot 3H_2O$[8c] were prepared according to literature methods.

Preparation of Bis[D-β-(2-pyridyl)-α-alaninato]cobalt(III) Nitrate Hemihydrate, $[Co(D\text{-}Pyrala)_2]NO_3 \cdot {}^1/_2H_2O$. $[Co(NH_3)_4CO_3]NO_3$ (0.75 g, 3.0 mmol) and D-PyalaH (1.00 g, 6.0 mmol) were dissolved in 40 mL of distilled water, and 0.3 g of activated charcoal was added. The solution was stirred at 85 °C for 20 h. The charcoal was filtered from the hot solution and washed with boiling water. The filtrate and wash solution were combined and evaporated to dryness. The glassy solid that formed was redissolved in a minimum of 80:20 $MeOH–H_2O$ and